# Photoactive Self-Shaping Hydrogels as Noncontact 3D Macro/Microscopic Photoprinting Platforms

Yue Liao, Ning An, Ning Wang, Yinyu Zhang, Junfei Song, Jinxiong Zhou, Wenguang Liu*

A photocleavable terpolymer hydrogel cross-linked with *o*-nitrobenzyl derivative cross-linker is shown to be capable of self-shaping without losing its physical integrity and robustness due to spontaneous asymmetric swelling of network caused by UV-light-induced gradient cleavage of chemical cross-linkages. The continuum model and finite element method are used to elucidate the curling mechanism underlying. Remarkably, based on the self-changing principle, the photosensitive hydrogels can be developed as photoprinting soft and wet platforms onto which specific 3D characters and images are faithfully duplicated in macro/microscale without contact by UV light irradiation under the cover of customized photomasks. Importantly, a quick response (QR) code is accurately printed on the photoactive hydrogel for the first time. Scanning QR code with a smartphone can quickly connect to a web page. This photoactive hydrogel is promising to be a new printing or recording material.
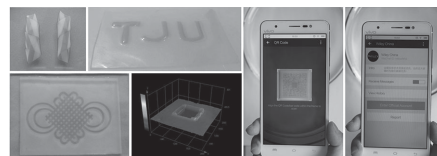
1. Introduction

Autonomous shape changing occurs frequently in nature. This phenomenon has recently been emulated to design reconfigurable soft materials with adaptivity and controllable geometrical shape.[1,2] In these fascinating self-changing materials, smart responsive hydrogels demonstrate the uniqueness to be programmed to adopt diverse shapes in response to a variety of stimuli.[3,4] The frequently used stimuli for triggering shape change include temperature, pH, redox, ion, and light.[5–11] Of these stimuli, light is particularly attractive, due to its distinct advantages over other triggers, such as remote, spatial, and temporal controllability.[12–15] To make photoresponsive hydrogels, light sensitive functional groups such as cinnamic acid, spiropyran, azobenzene, coumarin, and *o*-nitrobenzyl have to be incorporated into the cross-linked hydrophilic polymer network.[16–20] Upon light irradiation, the hydrophilicity or cross-linking density of hydrogels can be tuned by isomeric transformation or cleavage of photodegradable cross-linker, bringing about the macroscopic changes such as Young's modulus, swelling degree, and water diffusion.[21,22] Based on these modulable properties, photoresponsive hydrogels have been used in diverse applications like cells detachable substrate,[14] artificial muscle,[23] controllable drug delivery,[24] microfluidic system,[25] fabrication of rewritable microrelief,[26]

Y. Liao, Dr. N. Wang, Y. Zhang, J. Song, Prof. W. Liu
School of Materials Science and Engineering
Tianjin Key Laboratory of Composite and Functional Materials
Tianjin University
Tianjin 300072, China
E-mail: wgliu@tju.edu.cn
N. An, Prof. J. Zhou
State Key Laboratory for Strength and Vibration
of Mechanical Structures and School of Aerospace
Xi'an Jiaotong University
Xi'an 710049, China
Dr. N. Wang
National Technology Testing Center for Footwear (Wenzhou)
Wenzhou 325007, China

and spatiotemporally controllable 3D cell culture platform.[27] In fact, for a photocleavable chemical cross-linked hydrogel, the decross-linking degree will attenuate along its thickness as the light passes through its bulk, consequently resulting in gradient change in cross-linking density.[15] In this case, the gel was not completely eroded, but may become a light-processable soft and wet material by adjusting light exposure time and energy. On the other hand, most photolabile hydrogels undergo color change upon exposure to light.[17,20] In view of these light-induced switchable properties and unexplored application perspectives, we will design and synthesize a photoscissile o-nitrobenzyl derivative cross-linked hydrogel, and investigate the sophisticated control of self-changing in this study. Particularly, these light-active hydrogels will be explored as soft-wet paper for 3D macro/microscopic photoprinting; a quick response (QR) code (or 2D barcode) is encoded on the photocleavable hydrogel for the first time. We demonstrate that the image of the QR code can be scanned and decoded by a smartphone to quickly connect to a web page. It is expected that the photoactive hydrogel could be developed as an interesting printing or recording material.

2. Results and Discussion

2.1. Photocleavage of P(AAm-co-THMMA-co-NB526) (PATN) Hydrogels

In this work, we aimed to construct a photoresponsive hydrogel to realize light-triggered self-changing, photoprinting and decoding QR code. Thus, this photoresponsive hydrogel essentially acted as a robust matrix even if its cross-linking had been partially cleaved. Based on these design demands, we synthesized terpolymer hydrogels by copolymerizing acrylamide (AAm), N-[tris(hydroxymethyl)methyl] acrylamide (THMMA), and a photocleavable cross-linker, PEG526-methacrylate-4-(4-(1-acryloyloxyethyl)-2-methoxy-5-nitrophenoxy) butanoate (NB526). We noted that since NB526 is hydrophobic, two hydrophilic monomers, AAm and THMMA were included. In addition, AAm and THMMA are capable of forming self-hydrogen bonding.[14,28,29] Therefore, we can anticipate that the PATN hydrogels could keep their physical integrity and robustness after photoscission due to hydrogen bonding reinforcements from AAm and THMMA. Here, the monomer weight ratio of 1:1 (AAm/THMMA) was used taking into account its optimal integrated performance of hydrogels. Figure S2 (Supporting Information) reveals the successful preparation of PATN hydrogel, and its schematic network structure is depicted in Scheme 1.

An acetonitrile solution of NB526 (1.1×10^{-7} mol mL^{-1}) was irradiated with 365 nm UV light for different times. Photolysis was monitored by UV–vis spectroscopy (Figure 1a). As shown in the figure, the decreased absorption at 300 nm suggests the breakage of photolabile ester bond, and increased absorption at 245 and 375 nm implies the formation of photolysis product o-nitrosoacetophenone (Scheme 1).[30] To simplify the discussion, "UV irradiation" will specifically refer to exposing the hydrogel to 365 nm UV light in water for 15 min. In the attenuated total reflection Fourier transform infrared (AIR-FTIR) spectra of the PATN hydrogels before and after UV irradiation (Figure 1b), the band at 1520 cm^{-1}, attributable to NO$_2$ asymmetric stretch, decreases in the degraded hydrogel, evidencing that NO$_2$ groups have transformed into NO groups after the photocleavage of o-nitrobenzyl moiety upon UV light exposure.[31] Besides, no change in other peaks is observed, suggesting that PAAm and
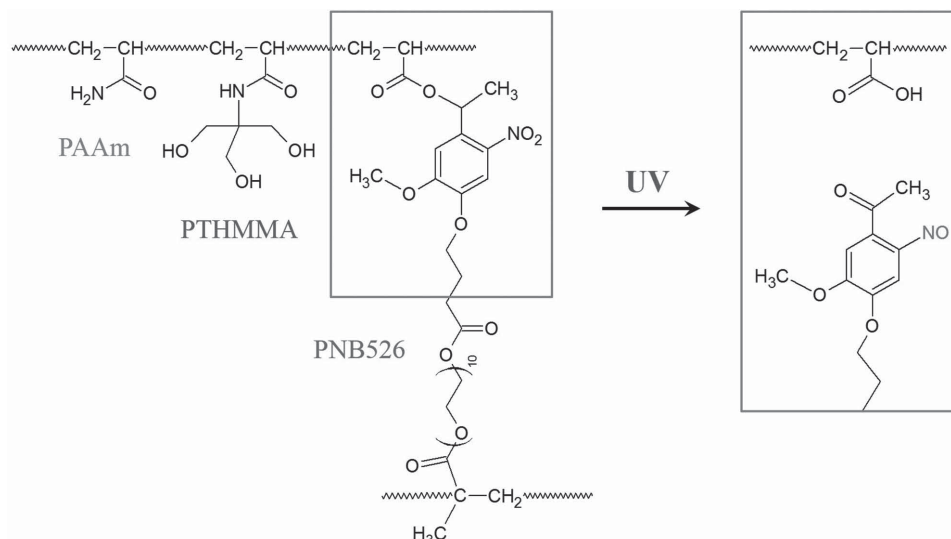
Scheme 1. Schematic molecular structure of PATN hydrogel and the cleavage of the photolabile moiety upon UV irradiation.
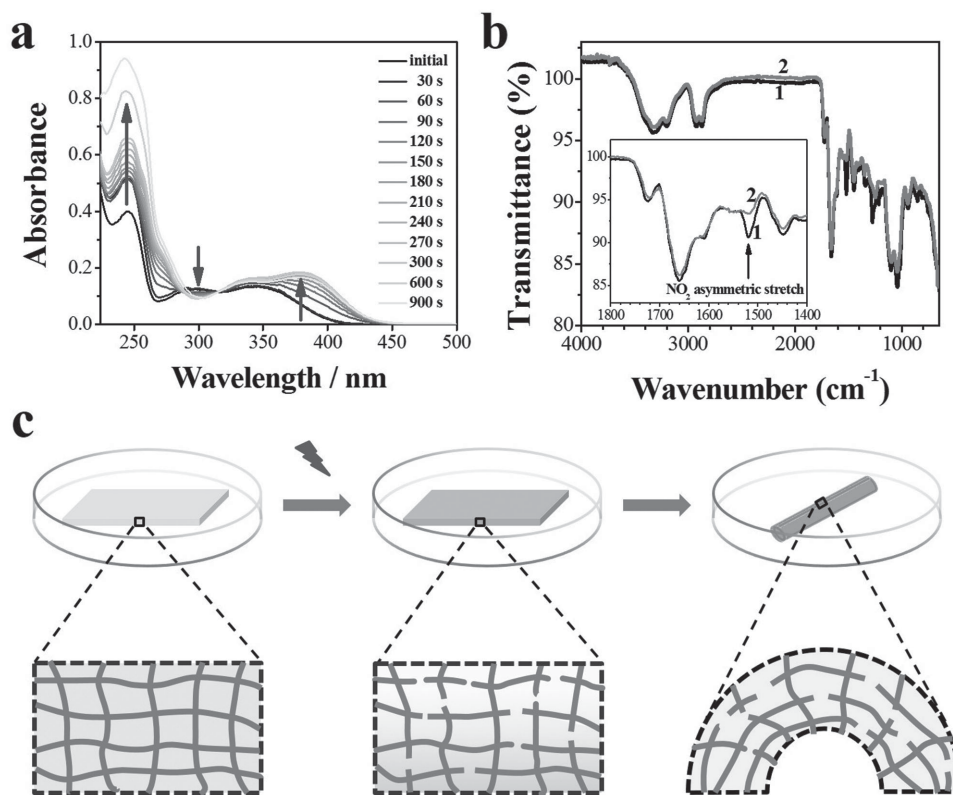
www.MaterialsViews.com

Figure 1. a) UV–vis spectra of NB526 cross-linker solution in acetonitrile (1.1×10^{-7} mol mL^{-1}) after different irradiation times. b) AIR-FTIR spectra of original PATN1-1-1 (line 1) and UV-exposed sample (line 2); the enlarged spectra from 1800 to 1400 cm^{-1} in the inset allows for a clear observation of change in O=N=O asymmetric stretch absorption peak prior and after UV light irradiation. c) Sketch illustrating underlying mechanism of UV-light-triggered self-shaping of PATN hydrogels.

PTHMMA in PATN hydrogel are not affected by irradiation (Figure 1b).

As demonstrated in the above analysis, the *o*-nitrobenzyl ester linkage in cross-linker NB526 could be cleaved by UV light irradiation. Nonetheless, we found that the whole PATN hydrogel was not completely disintegrated due to the partial chain-cleavage in the network. Macroscopically, the changes in the swelling and mechanical properties of PATN hydrogels were observed (Figure S3, Supporting Information). It is shown that the equilibrium water content (EWC) of any irradiated sample is higher than that of its original one (Figure S3a, Supporting Information). The swelling properties of hydrogels are positively related to EWC values;[13] thus the increased EWCs reflect the partial decross-linking of the hydrogel network due to the UV-light-induced photocleavage of *o*-nitrobenzyl ester bonds. As expected, with an increment of NB526 cross-linker contents, the EWCs of both the untreated and the UV-treated hydrogels show a declining trend owing to increased compactness of network (Figure S3a, Supporting Information). To quantify some structural parameters of hydrogel network, especially the cross-linking density, the average molecular weight between cross-links (M_c) calculated was shown in

Table S1 (Supporting Information). The results indicate that each M_c value of primary sample is lower than its UV-irradiated one; correspondingly the cross-linking density of the PATN hydrogel is reduced after experienced UV irradiation. Also, it is evident that the M_c values increased with the decrease of NB526 cross-linker content for the two groups of PATN hydrogels before and after UV stimulation, indicating the consistency with aforementioned results.

The UV irradiation is also shown to result in the decrease in the densities of all hydrogels since the decrosslinking leads to the increased hydration of network (Figure S3b, Supporting Information). The effect of UV irradiation on the mechanical properties of PATN hydrogels was also checked. Figure S3c,d (Supporting Information) shows that partial degradation of NB526 cross-linker caused by UV irradiation contributes to the reduction in both the tensile strengths and Young's moduli of all the selected samples; nevertheless, the cleaved hydrogels were mechanically strong enough for handling. In view of their higher strengths, PATN1-1-1 and PATN3-3-2 hydrogels were selected for the subsequent experiments.

As aforementioned, UV-light-induced breakage of NB526 cross-linker is accompanied with water uptake

and swelling of network, resulting in density and modulus reduction. Furthermore, for this photocleavable chemical cross-linked hydrogel, the decross-linking extent attenuates along its depth direction under UV light irradiation, accordingly causing a gradient change of cross-linking density.[15] As a result, the photocleaved hydrogel is in the nonequilibrium state within short time, which would generate spontaneous asymmetric swelling, thus triggering self-rolling or self-shaping to reach a new equilibrium state. The underlying mechanism is depicted in Figure 1c.

2.2. Light-Induced Self-Shaping of PATN Hydrogels

We can envision that irradiating a uniform hydrogel membrane by UV light through a photomask would attain a heterogeneous hydrogel network with patterned distribution of irradiated and nonirradiated regions. The irradiated region is also nonuniform with gradient of cross-linking density and thus swelling ratio through thickness due to the attenuation of light intensity along the depth direction. Therefore, a hydrogel strip with difference in swelling ratio through thickness would bend or fold to accommodate the mismatch of strain. The nonirradiated region constrains and accompanies the bending and folding of the irradiated region, leading to the evolution of a 2D hydrogel sheet into a programmable 3D structure to release the generated internal stress. It is worth noting that the film thickness of 500 μm is chosen to achieve a good balanced performance of self-rolling and manipulating properties (Figure S4, Supporting Information). Next, we exploited this principle to design and fabricate a variety of self-folding structures.

Mimicking the petals of a flower with the hydrogel film in response to UV light stimulus is shown in Figure 2a–c. The central area of the starting hydrogel (Figure 2a) was blocked with a photomask before irradiation. Upon UV light irradiation, the gel began to curl up to a hexagon (Figure 2b). This transformation is perpetual and irreversible—the shape could be maintained in water for 6 months or longer time. Clearly, the UV-irradiated area became yellowish immediately, while the unirradiated area remained unchanged. Interestingly, inorganic salt solution could bring about a reversible folding–unfolding transition of the "flower". Immersed in 2 wt% CaCl$_2$ solution, the rolled "petals" unfolded to a certain open angle (Figure 2c), assuming a blooming flower. A possible reason is that the negatively charged COO$^-$ groups generated under UV light were shielded with addition of salt, resulting in somewhat deswelling of the PATN hydrogel.[32] Moreover, there is a gradient of shrinkage—the deswelling degree tends to reduce along the thickness due to light-triggered continuously decreased conversion of COO$^-$ groups with the increase in depth. This asymmetric shrinking pulls back the

closed "petals" with a slant angle. Besides CaCl$_2$, a similar phenomenon was also observed in aqueous solutions of NaCl, KCl, FeCl$_2$, and PBS, etc. Soaking in deionized water again, the six "petals" could refold and assumed the same closed state as that shown in Figure 2b. In this case, with salt leaking out of network, the PATN hydrogel regained its swelling state, inducing another cycle of folding.

Figure 2e depicts two chiral helices of hydrogels formed from the slender hydrogel strips by region-selective UV light irradiation. To obtain different chiralities, the gel strips were covered with two distinct striped photomasks, one with 45° slant angle of stripes and the other with 135° slant angle of stripes. Upon UV light illumination, one hydrogel strip blocked with 45° stripe photomask rolled up into a left-handed helix; while the other 135° stripe mask-covered gel strip self-shaped into a right hand helix. An explanation is that in UV-irradiated areas, the NB526 is cleaved, which results in a gradient increase of cross-linking density along the light transmission; as a consequence, internal stress is generated in the network to push strips to curl up backward the UV-light-irradiated face parallel to the stripes due to larger swelling on the exposed surface. Since curling toward one direction occurred at multiple separate regions on one single piece of hydrogel, a twisting force was resulted, eventually contributing to the formation of a helix.[33] To achieve more fascinating shape changing, a hydrogel strip was illuminated with UV light on two specific regions (Figure S5, Supporting Information). As shown in the figure, two opposite side surfaces of the hydrogel were respectively covered with one parallelogram stripe-patterned photomask with the slant angles of 45°. After UV light irradiation for 15 min, two light illuminated-areas began to twist toward opposite directions owing to the photolysis-induced different swelling anisotropy; then the ends of the twisted strip were joined together manually to form a Mobius Band loop which has a surface with only one side and only one boundary.

To fully understand the underlying mechanism of self-folding behaviors of patterned hydrogels, we built a continuum model and used a finite element method (FEM) to model the self-folding processes (Figure 2d,f–h). The simulations of the curling of flower petals and rolling of helices were performed in a commercial software ABAQUS by programming a user material subroutine for swelling of hydrogels. The simulation results captured and unveiled the experimental observations: the curling of petals (Figure 2d; Movie S1, Supporting Information) and rolling of helices (Figure 2f–h; Movies S2 and S3, Supporting Information) were caused by the bending of the irradiated regions, which was ascribed to the gradient of swelling ratio across the thickness of the material. This mechanism of formation of helices through continuous bending was different from the buckling
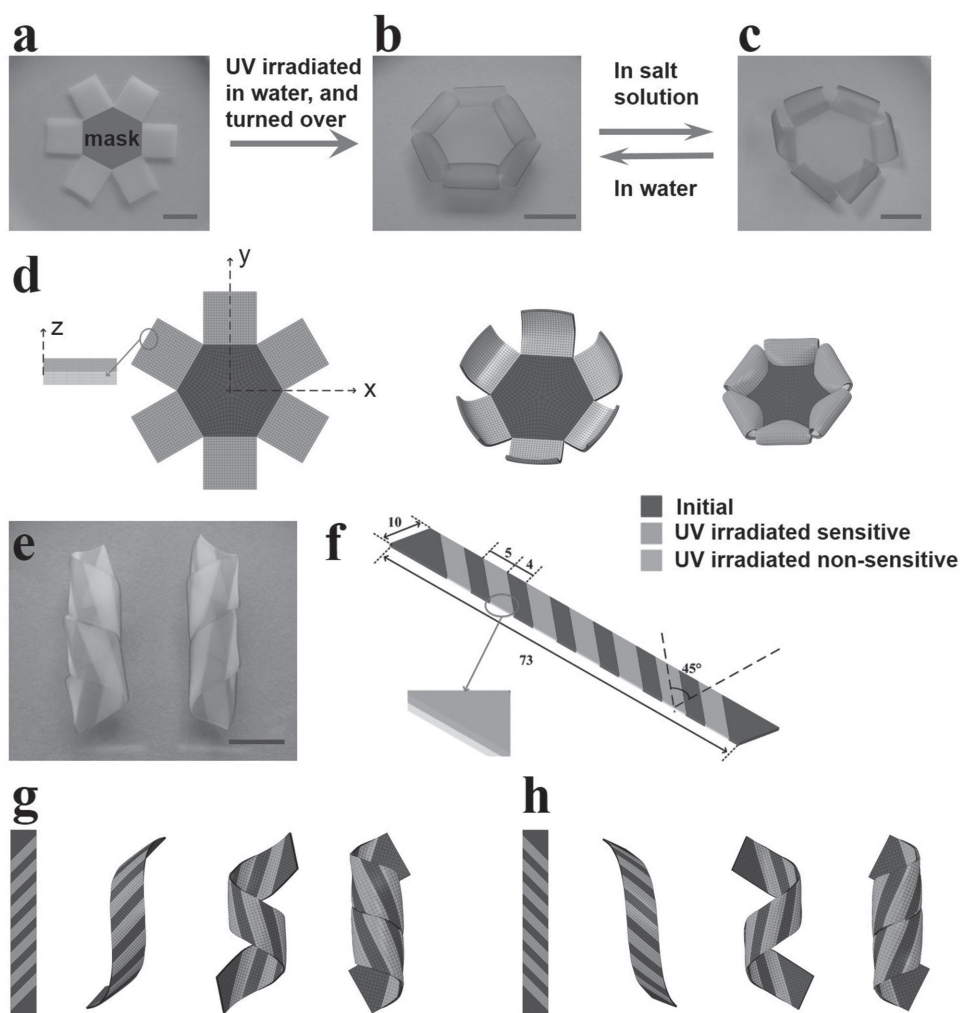
2132

Macromolecular
Journals

Macromol. Rapid Commun. **2015**, *36*, 2129–2136

© 2015 WILEY-VCH Verlag GmbH & Co. KGaA, Weinheim

Materials
Views

www.MaterialsViews.com

Figure 2. Experimental observation and FEM simulation of UV-light-triggered self-shaping of PATN hydrogels. a) A flat PATN1-1-1 hydrogel sheet with six petals was covered with a photomask in the center; b) upon exposing UV light, the gel self-folded into a hexagon with six tube edges, which was then turned over for photographing; c) immersing in salt solution, the tube edge of the hexagon unfolded into a blooming flower and b) reversibly folded back into "close" state after removing salt. d) FEM simulation of self-folding of a hexagon. e) A slender hydrogel strip separately covered with a photomask with 45° slant angle of stripes (corresponding to g) and 135° slant angle of stripes (corresponding to h) rolled up into a left-handed and right-handed helix upon UV light illuminating. f–h) FEM simulation of the transformation of helices. The blue regions are the initial materials unaffected by UV irradiation, and the green ones were exposed to UV illumination. The gradient of material properties across the thickness of the irradiated region was simplified by a bilayer denoted by "UV-irradiated sensitive" and "UV-irradiated nonsensitive". A patterned hydrogel sheet self-folded into a 3D configuration through continuous bending of the material. Scale bar = 10 mm.

mechanism reported previously.[33] For the formation of helices through buckling of hydrogel sheets, the hydrogel composites had only in-plane structure difference and were uniform across the thickness. It makes no difference for a hydrogel strip with a slant angle + θ illuminated from top and a strip with slant angle $180° - \theta$ but illuminated from bottom. The generated in-plane forces drove the buckling of the strip, and the strip could buckle either upward or downward with equal probability. So, the chirality of helix mediated by buckling is undetermined with equal probability of left-hand and right-hand chiralities.[33] In contrast, for our photoactive hydrogel

with structure difference or gradient change of cross-linking density across the thickness, nonuniform stresses were generated and the internal stresses were released through bending. For a hydrogel strip of this type, light illumination from top and bottom was of course different. The bending direction induced by UV irradiation was well determined in this case, and the side with larger swelling ratio was always convex while the side with smaller swelling ratio was always concave. Our additional simulations predicted that stripes with a slant angle less than 90° always rolled into left-hand helix, while stripes with a slant angle more than 90° could attain right-hand

helix. A brief description of the theory and model is provided in the Supporting Information.

Moreover, we noted that if the two sides of the hydrogel strip were totally exposed to UV light, no curling or folding occurred due to symmetric and homogenous swelling of network under this condition. To highlight the indispensable role of NB526 cross-linker in this light responsive self-changing hydrogel, a light-insensitive cross-linker polyethylene glycol (M_n = 575) was copolymerized with AAm and THMMA to form a hydrogel P(AAm-co-THMMA-co-PEGDA575). Upon exposure to UV light, the P(AAm-co-THMMA-co-PEGDA575) hydrogel sheet remained unchanged both in shape and color (Figure S6, Supporting Information), suggesting the photocleavable cross-linkage was the main factor for occurrence of self-rolling. In addition, we found that in the absence of either AAm or THMMA, the hydrogel obtained could not demonstrate satisfactory mechanical properties or self-shaping behaviors.

2.3. Noncontact 3D Macro/Microscopic Photoprinting

The above results demonstrated that UV light irradiation resulted in the increased swelling of PATN hydrogels, and anisotropic swelling can generate diverse transformers. We can envision that if UV light passes through tiny openings to irradiate the surface of PATN hydrogel, small protrusions could be created.[34,35] Based on this principle, we hypothesize that this photoresponsive hydrogel can be applied to 3D macroscopic and microscopic photoprinting by simply tuning the pattern size of photomask. A PATN hydrogel disk immersed in water was covered with a concentric photomask, and illuminated with UV light. When the gel was taken out of water, we found that a dark yellow round protrusion with the maximum diameter of 18 mm was generated in the center of the hydrogel (Figure 3a). It is obvious that the embossed yellow central protrusion is originated from local swelling of the hydrogel caused by UV-light-induced cleavage of NB526 cross-linker. Likewise, three convex capital letters "TJU" (acronym of Tianjin University) are precisely printed on the surface of PATN hydrogel with UV light illuminating to the hollow TJU photomask (Figure 3b). In the same way, English and Chinese versions of a poem could be precisely printed on the gel surface using two outline character photomasks (Figure S7, Supporting Information).

Also, we can print delicate Chinese knot on the surface of PATN hydrogels by UV light irradiation. Intriguingly, we can achieve intaglio printing and relief printing by using tailored photomasks. As depicted in Figure 3c, when an open lined Chinese knot mask was used, the transmitted UV light led to a convex image due to the swelling of contour lines. In contrast, while UV light illuminated to solid-lined Chinese knot
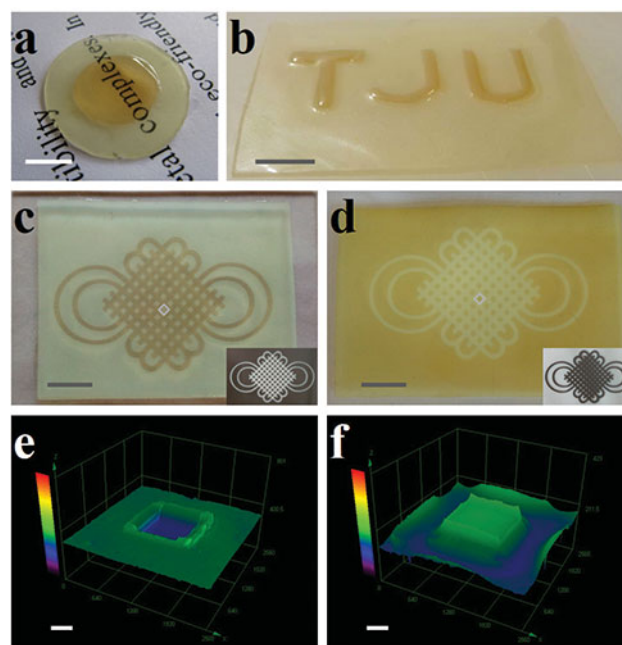

Figure 3. a) A yellow round protrusion was formed in the center of PATN3-3-2 hydrogel disk when UV light illuminated through a concentric photomask. b) Convex capital letters "TJU" (acronym of Tianjin University) were accurately printed on the surface of PATN3-3-2 hydrogel with UV light illuminating. c) Convex and d) concave Chinese knots were separately printed on the PATN1-1-1 hydrogel surface while UV light illuminated to open (inset image in c) and solid (inset in d) contour lines of photomasks. e,f) 3D images of a square unit respectively selected from the middle of convex and concave knots taken by 3D measuring laser microscope. a–d): Scale bar = 10 mm; e, f): Scale bar = 400 μm.

mask, the whole knot was lightproof, and the areas surrounding the contour lines were irradiated to degradation. Under this condition, the surrounding regions were protruded due to the occurrence of the local swelling. As a consequence, a concave Chinese knot image was formed (Figure 3d). The concave characters in microscale could also be successfully printed on the gel surface using a lightproof photomask template (Figure S8, Supporting Information). Figure 3e,f displays the 3D square units selected from the middle of knots taken by 3D measuring laser microscope. An altitude difference of about 90 μm is resulted in these two 3D units, reflecting visually the printing of convex and concave Chinese knots.

As demonstrated above, PATN hydrogel underwent color change when irradiated with UV light. That reminded of encoding QR code on the gel surface. We designed a photomask using the QR code of Wiley China as a template by Auto CAD. On the mask, the white and dark regions are the light-permeable and lightproof ones, respectively (Figure 4a). This mask was placed perpendicular to the top of a PATN gel sheet. Upon UV light irradiation, the QR code pattern was faithfully
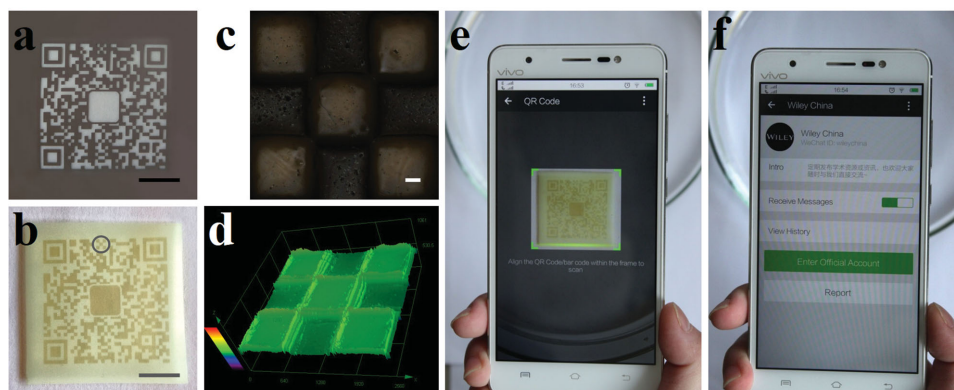
2134

![Macromolecular Journals]

Macromol. Rapid Commun. **2015**, *36*, 2129–2136
© 2015 WILEY-VCH Verlag GmbH & Co. KGaA, Weinheim

![Materials Views]
www.MaterialsViews.com

Figure 4. a) Covered with the corresponding template photomask, b) the QR code of Wiley China was precisely printed on the surface of PATN1-1-1 hydrogel. c,d) 3D microscopic images of the selected circle region from QR code on the gel. e,f) Scanning QR code on the gel surface and accessing Wiley China website using a smartphone. a, b): Scale bar = 10 mm; c): Scale bar = 200 μm.

printed on the surface of PATN gel with light-exposed dark yellow patterns and unexposed light yellow patterns (Figure 4b). We scanned the QR code printed on the gel immersed in water with a smartphone through a software of WeChat. Excitingly, the official website of Wiley China was quickly accessed on the screen of the phone (Figure 4e,f; Movie S4, Supporting Information). It is worthwhile to note that apart from color change, the altitude of light irradiated regions is enhanced due to the local swelling, compared to that of the unexposed areas. The altitude difference of the patterns is about 170 μm (Figure 4c,d). Thus, it is actually a 3D QR code. We can anticipate that more information could be photoencoded in this hydrogel with simplicity and convenience, holding a great potential as a new recording material.

3. Conclusion

In summary, to mimic the self-changing behaviors of living systems, a photoresponsive *o*-nitrobenzyl derivative cross-linked hydrogel comprising AAm and THMMA, two typical hydrophilic monomer units, was designed and fabricated. The photoresponsive hydrogels exhibited automatic shape changing without sacrificing the physical integrity due to spontaneous asymmetric swelling of network due to the gradient decross-linking density through its thickness resulted from UV-light-induced cleavage of NB526 cross-linkages. This photosensitive hydrogel enabled the formation of programmable pattern and multiple geometric shapes driven by region-selective UV irradiation. We performed numerical simulations and found a good agreement between experiment observation and simulation. We elucidated the bending mechanism ascribed to the gradient of material properties across the thickness of hydrogels. We demonstrated that this photosensitive

hydrogel could find diverse attractive applications as a 3D macro/microscopic photoprinting platform to accurately duplicate the characters and images without contact, simply by UV light illuminating the customized photomasks. We realized, for the first time, precise printing of QR code (or 2D barcode) on the photograded hydrogel, and scanning the QR code with a smartphone enabled quick link to a desired web page. This novel photoactive hydrogel holds a great potential as an interesting printing or recording material.

Supporting Information

Supporting Information is available from the Wiley Online Library or from the author.

[1] L. Ionov, *Adv. Funct. Mater.* **2013**, *23*, 4555.
[2] J.-H. Na, A. A. Evans, J. Bae, M. C. Chiappelli, C. D. Santangelo, R. J. Lang, T. C. Hull, R. C. Hayward, *Adv. Mater.* **2015**, *27*, 79.
[3] H. Thérien-Aubin, Z. L. Wu, Z. Nie, E. Kumacheva, *J. Am. Chem. Soc.* **2013**, *135*, 4834.
[4] J. Kim, J. A. Hanna, M. Byun, C. D. Santangelo, R. C. Hayward, *Science* **2012**, *335*, 1201.

[5] V. Stroganov, S. Zakharchenko, E. Sperling, A. K. Meyer, O. G. Schmidt, L. Ionov, *Adv. Funct. Mater.* **2014**, *24*, 4357.

[6] C. Yoon, R. Xiao, J. Park, J. Cha, T. D. Nguyen, D. H. Gracias, *Smart Mater. Struct.* **2014**, *23*, 094008.

[7] L. Liu, N. Wang, Y. Han, Y. Li, W. Liu, *Macromol. Rapid Commun.* **2014**, *35*, 344.

[8] Y. Han, T. Bai, Y. Liu, X. Zhai, W. Liu, *Macromol. Rapid Commun.* **2012**, *33*, 225.

[9] T. Bai, Y. Han, P. Zhang, W. Wang, W. Liu, *Soft Matter* **2012**, *8*, 6846.

[10] Y. Han, T. Bai, W. Liu, *Sci. Rep.* **2014**, *4*, 5815.

[11] Y. Liu, J. K. Boyles, J. Genzer, M. D. Dickey, *Soft Matter* **2012**, *8*, 1764.

[12] I. Tomatsu, K. Peng, A. Kros, *Adv. Drug Deliv. Rev.* **2011**, *63*, 1257.

[13] N. Wang, J. Zhang, L. Sun, P. Wang, W. Liu, *Acta Biomater.* **2014**, *10*, 2529.

[14] N. Wang, Y. Li, Y. Zhang, Y. Liao, W. Liu, *Langmuir* **2014**, *30*, 11823.

[15] A. M. Kloxin, M. W. Tibbitt, A. M. Kasko, J. A. Fairbairn, K. S. Anseth, *Adv. Mater.* **2010**, *22*, 61.

[16] R. Kumar, S. R. Raghavan, *Soft Matter* **2009**, *5*, 797.

[17] J. E. Stumpel, B. Ziółkowski, L. Florea, D. Diamond, D. J. Broer, A. P. H. J. Schenning, *ACS Appl. Mater. Interfaces* **2014**, *6*, 7268.

[18] J. Shi, B. Wang, H. Du, *Colloid Polym. Sci.* **2014**, *292*, 1217.

[19] Y. Zhang, L. Ionov, *Langmuir* **2015**, *31*, 4552.

[20] F. Yanagawa, T. Mizutani, S. Sugiura, T. Takagi, K. Sumaru, T. Kanamori, *Colloids Surf. B Biointerfaces* **2015**, *126*, 575.

[21] M. Micic, Y. Zheng, V. Moy, X.-H. Zhang, F. M. Andreopoulos, R. M. Leblanc, *Colloids Surf. B Biointerfaces* **2002**, *27*, 147.

[22] G. Filipcsei, K. Sumaru, T. Takagi, T. Kanamori, M. Zrinyi, *J. Mol. Liq.* **2014**, *189*, 63.

[23] Y. Takashima, S. Hatanaka, M. Otsubo, M. Nakahata, T. Kakuta, A. Hashidzume, H. Yamaguchi, A. Harada, *Nat. Commun.* **2012**, *3*, 1270.

[24] Y. Qiu, K. Park, *Adv. Drug Deliv. Rev.* **2012**, *64*, 49.

[25] S. R. Sershen, G. A. Mensing, M. Ng, N. J. Halas, D. J. Beebe, J. L. West, *Adv. Mater.* **2005**, *17*, 1366.

[26] A. Szilágyi, K. Sumaru, S. Sugiura, T. Takagi, T. Shinbo, M. Zrínyi, T. Kanamori, *Chem. Mater.* **2007**, *19*, 2730.

[27] A. M. Kloxin, A. M. Kasko, C. N. Salinas, K. S. Anseth, *Science* **2009**, *324*, 59.

[28] X. Dai, Y. Zhang, L. Gao, T. Bai, W. Wang, Y. Cui, W. Liu, *Adv. Mater.* **2015**, *27*, 3566.

[29] N. Saito, T. Sugawara, T. Matsuda, *Macromolecules* **1996**, *29*, 313.

[30] P. Sobolčiak, M. Špírek, J. Katrlík, P. Gemeiner, I. Lacík, P. Kasák, *Macromol. Rapid Commun.* **2013**, *34*, 635.

[31] K. Peng, I. Tomatsu, B. van den Broek, C. Cui, A. V. Korobko, J. van Noort, A. H. Meijer, H. P. Spaink, A. Kros, *Soft Matter* **2011**, *7*, 4881.

[32] H. Ferenc, T. Ichiji, J. B. Peter, *Biomacromolecules* **2000**, *1*, 84.

[33] Z. L. Wu, M. Moshe, J. Greener, H. Therien-Aubin, Z. Nie, E. Sharon, E. Kumacheva, *Nat. Commun.* **2013**, *4*, 1586.

[34] C. Xue, D. Y. Wong, A. M. Kasko, *Adv. Mater.* **2014**, *26*, 1577.

[35] D. Y. Wong, D. R. Griffin, J. Reed, A. M. Kasko, *Macromolecules* **2010**, *43*, 2824.